

Supporting Information

One action, two benefits: Improving the performance of lithium-sulfur battery with a poly(ionic liquid)

*Sixin Jia^{‡a}, Rui Wang^{‡a}, Fengquan Liu^{*b}, Hong Huo^a, Jianjun Zhou^{*a}, Lin Li^{*ab}*

^a Beijing Key Laboratory of Energy Conversion and Storage Materials, College of Chemistry, Beijing Normal University, Beijing 100875, China

^b College of Textiles & Clothing, Qingdao University, Qingdao 266071, China

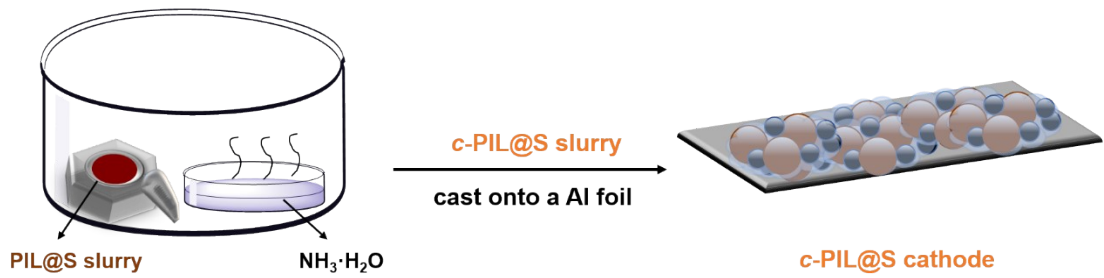


Fig. S1. Schematic diagram of preparing *c*-PIL@S composite cathode.

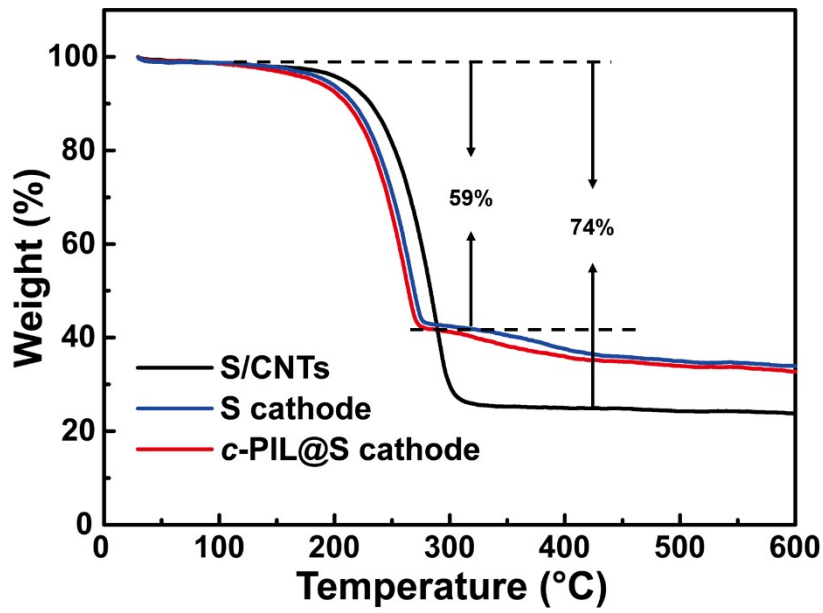


Fig. S2. TGA profiles of S/CNTs, blank S cathode and *c*-PIL@S cathode.

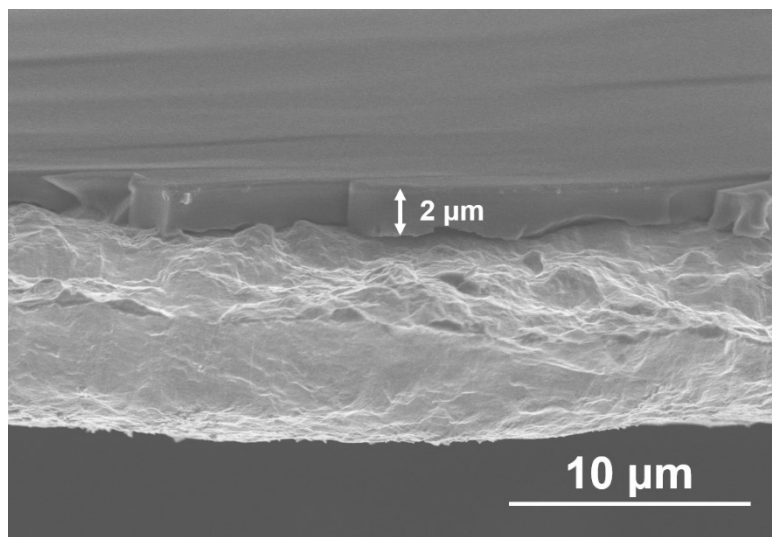


Fig. S3. Cross-sectional morphology of PIL@Cu.

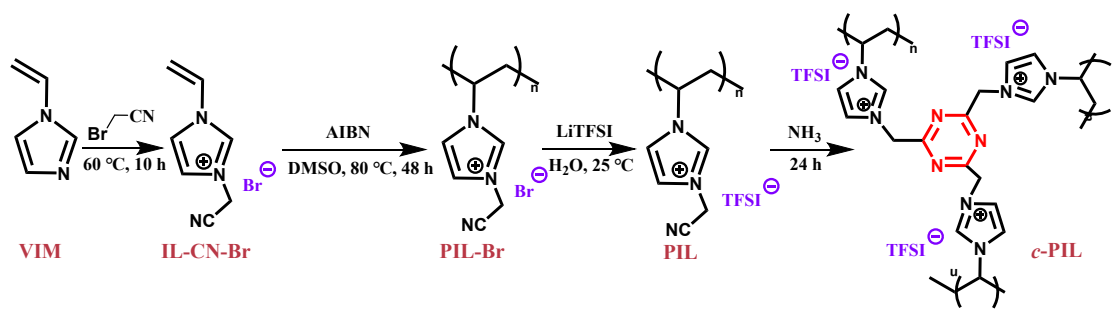


Fig. S4. The synthetic route of the PIL and *c*-PIL.

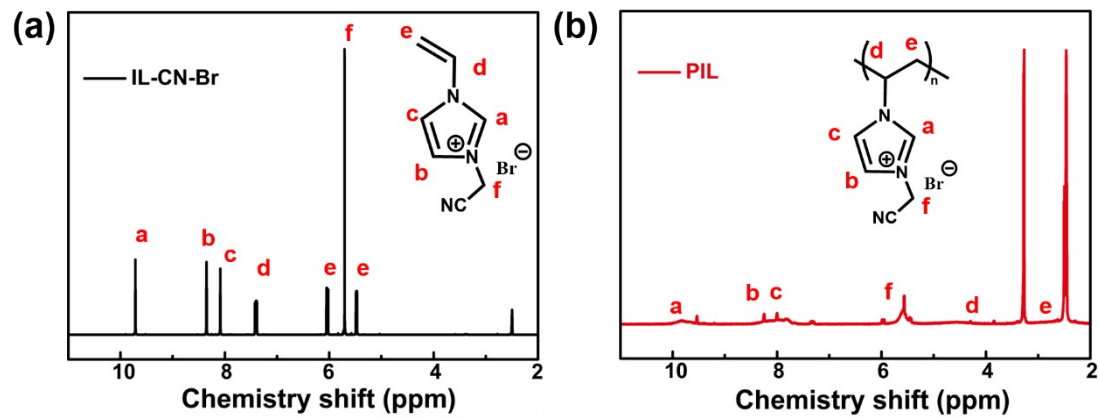


Fig. S5. ¹H NMR spectra of (a) IL-CN-Br and (b) PIL.

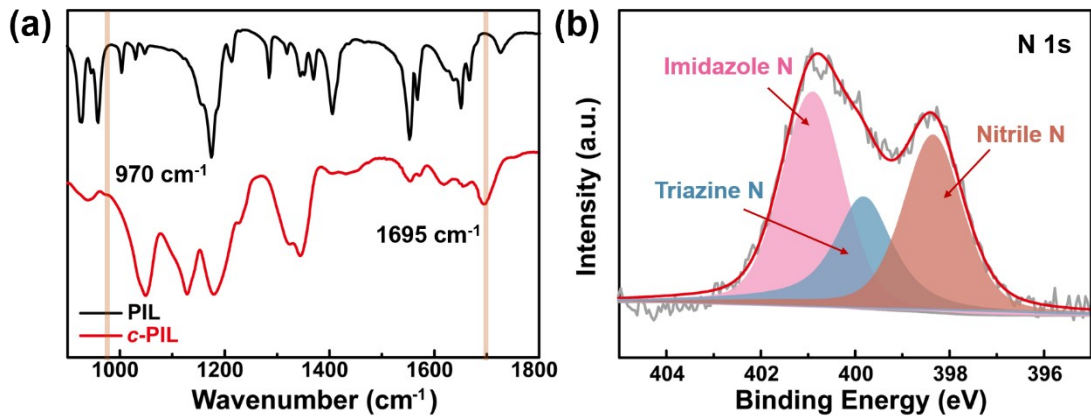


Fig. S6. (a) FTIR spectra of PIL (black line) and *c*-PIL (red line); (b) The XPS spectrum of N 1s for *c*-PIL.

In order to verify the structure variation of nitrile groups, FTIR spectra were used to characterize the PIL before and after NH₃ vapor treatment. For the triazine group, there exist two characteristic bands: one at 970 cm⁻¹ (attributed to C-N bond), another at 1695 cm⁻¹ (attributed to C=N bond). As shown in Fig. S6a, the two characteristic bands don't appear in PIL, but they are observed in *c*-PIL, indicating that PIL has been cross-linked with triazine. In addition, in the N 1s spectrum of X-ray photoelectron spectroscopy (XPS), besides the peaks at 400.9 eV (N on imidazole) and 398.4 eV (N on -CN group), a peak at 399.8 eV (N on triazine) can be split (Fig. S6b), which further verify the cross-linking of PIL with triazine.

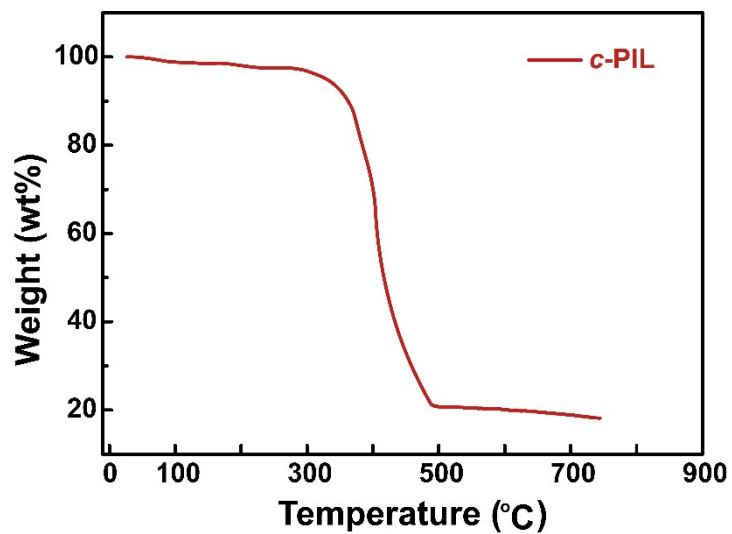


Fig. S7. The TGA curve of the *c*-PIL.

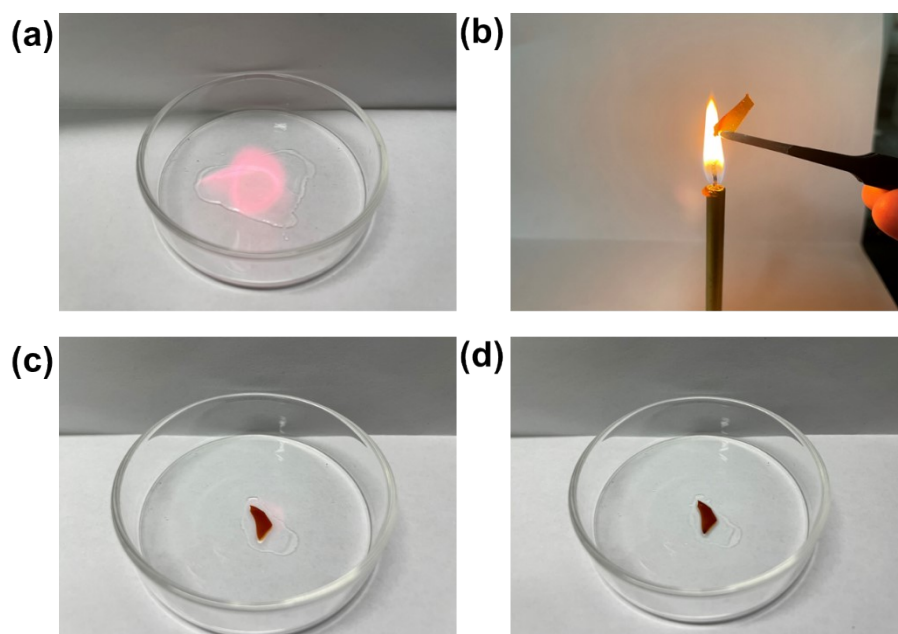


Fig. S8. Photographs demonstrating flammable behavior of (a) liquid electrolyte and (b-d) *c*-PIL.

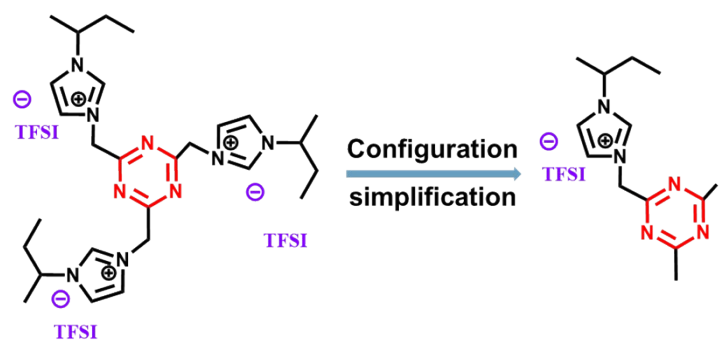


Fig. S9. Simplified configuration of *c*-PIL for calculation.

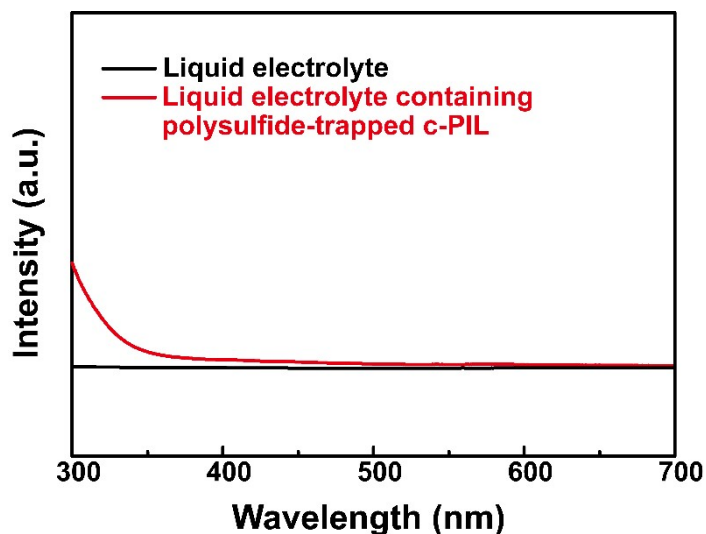


Fig. S10. The releasing of polysulfide in liquid electrolyte containing polysulfide-absorbed *c*-PIL.

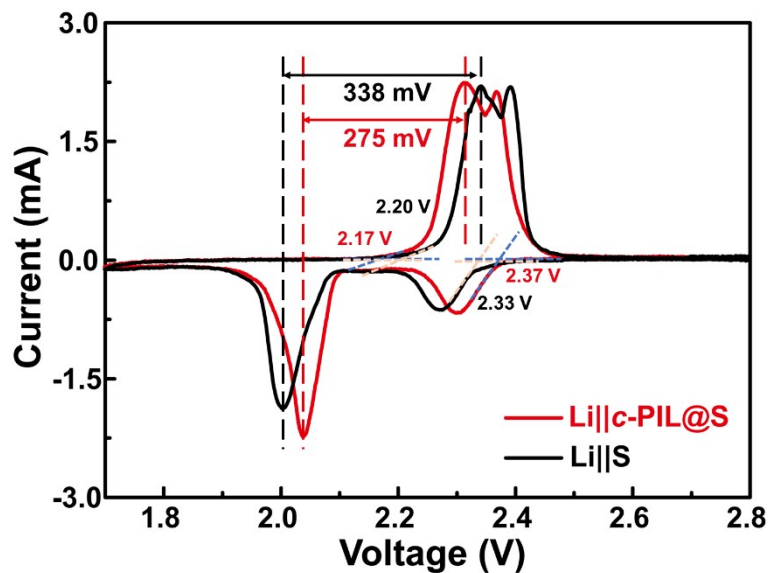


Fig. S11. CV curves of $\text{Li}||\text{S}$ and $\text{Li}||\text{c-PIL}@\text{S}$ batteries at 0.1 mV S^{-1} .

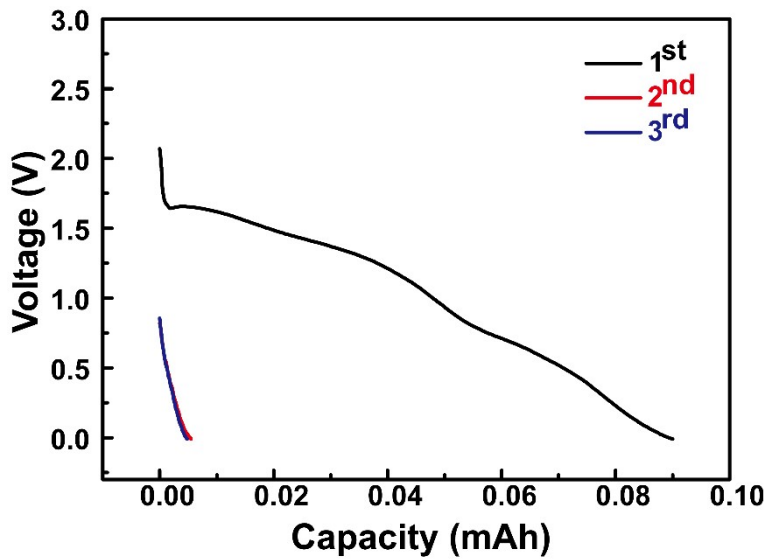


Fig. S12. The discharge curves of Li||PIL@Cu battery in the first 3 cycles at 0.01 mA cm^{-2} .

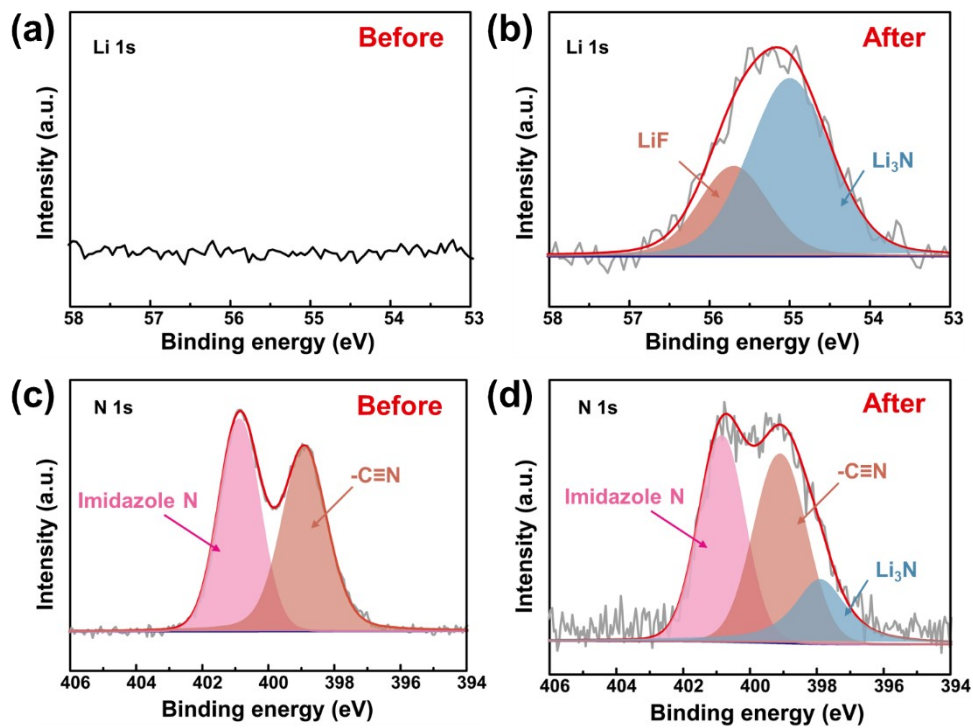


Fig. S13. XPS spectra of PIL removed PIL@Cu foil surface. Li 1s spectra (a) before and (b) after Li deposition; N 1s spectra (c) before and (d) after Li deposition.

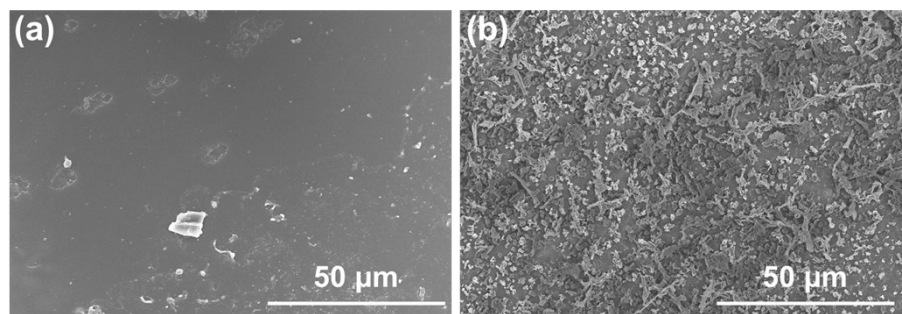


Fig. S14. SEM images of the Li anode surface from (a) Li||PIL@Cu and (b) Li||Cu batteries after 20 cycles.

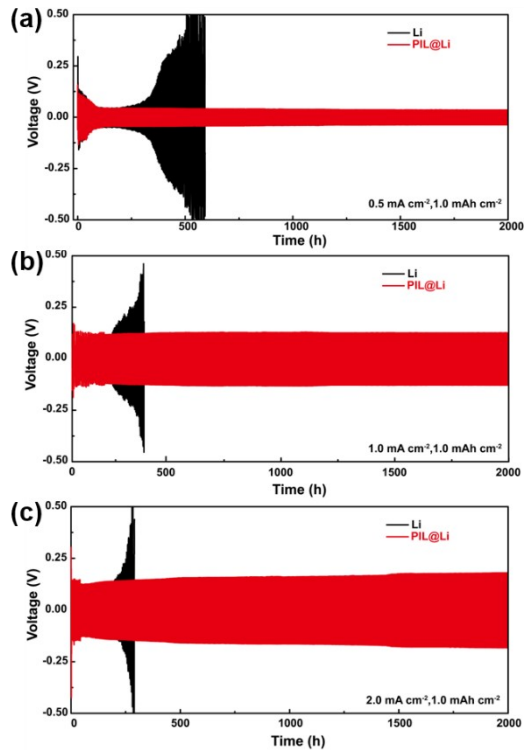


Fig. S15. Lithium stripping/platting curves of $\text{Li}||\text{Li}$ and $\text{Li}@\text{PIL}||\text{PIL}@\text{Li}$ symmetric batteries with different current densities. (a) 0.5 mA cm^{-2} , (b) 1.0 mA cm^{-2} and (c) 2.0 mA cm^{-2} .

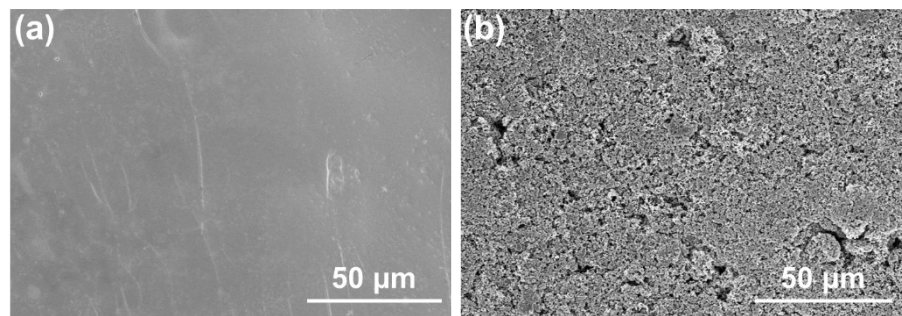


Fig. S16. The surface morphology of Li anode from (a) Li@PIL||PIL@Li and (b) Li||Li batteries after 100 cycles.

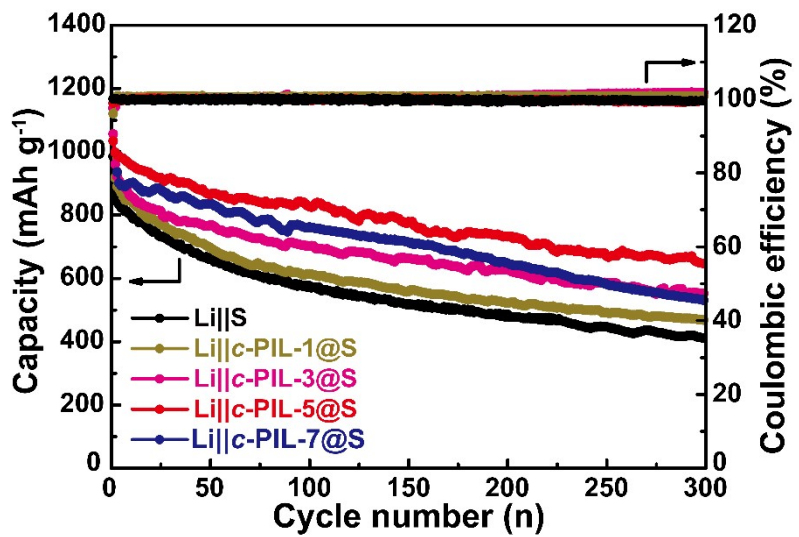


Fig. S17. The cycle performance of the $\text{Li}||\text{c-PIL}@\text{S}$ batteries with different contents of c-PIL .

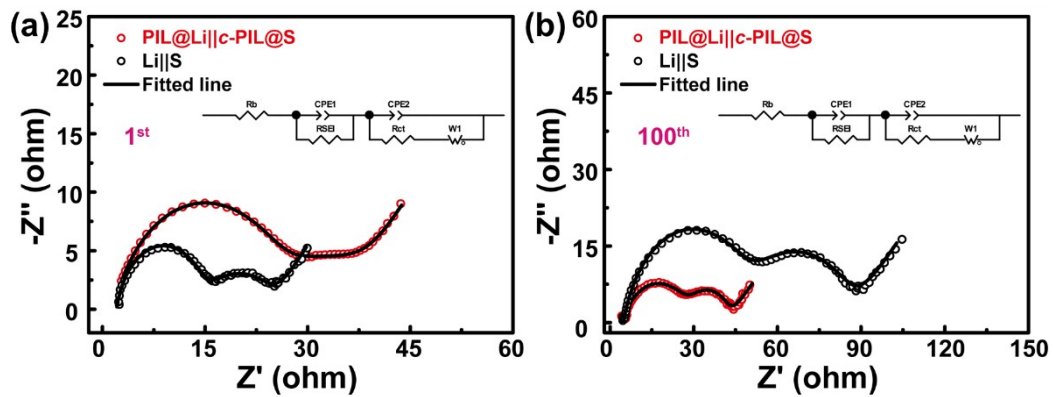


Fig. S18. The EIS spectra of (a) Li||S and (b) PIL@Li||c-PIL@S batteries after the 1st and 100th cycle.

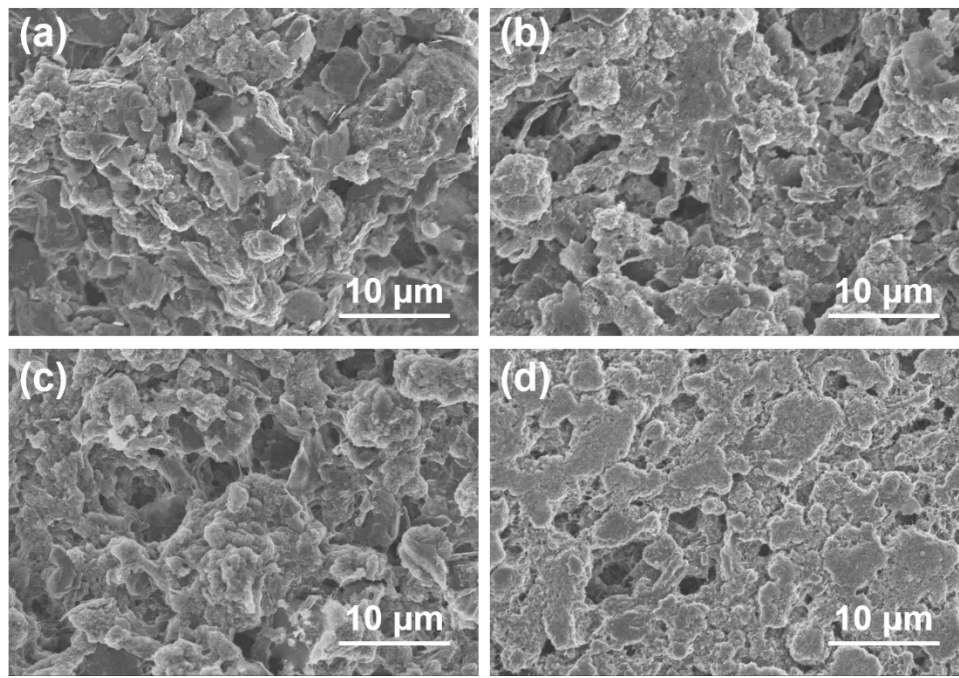


Fig. S19. Surface morphologies of the cathode. Cathodes of (a) the initial and (b) the 50th cycle from the Li||c-PIL@S battery; (c) the initial and (d) the 50th cycle from the Li||S battery.

Table S1. Electrochemical performance for the Li-S batteries reported in recent years.

Electrodes	Sulfur loading (mg cm ⁻²)	Sulfur content (%)	E/S ratio ($\mu\text{L mg}^{-1}$)	Current density (C)	Initial Capacity (mAh g ⁻¹)	Capacity decay (%) / Cycles/ Decay rate(%)	CE (%)	Ref.
CCSN-S	1.1-1.3	/	/	1.0	828.0	41.4/500/0.083	97.2	[S1]
DIT/S	1.5	49	15	0.2	1092.1	38.6/400/0.097	>97%	[S2]
PPy-SO ₄ /S	2.5	69.41	12	0.2	1149.1	44.3/300/0.148	/	[S3]
S@c-LSO-TPG	3.3	/	15.2	0.1	~1200	29.9/100/0.299	97.4	[S4]
S-co-poly-LCNT	1.0	58	/	0.5	1040	41.3/200/0.2065	~92	[S5]
CoNP-VSA@CF	1.22	/	20	0.5	1105	34.1/500/0.068	/	[S6]
3D-NOPC@S	1.0	70.1	32	0.5	~900	21.9/200/0.109	/	[S7]
S-TVTCSi ₄ -CNT _{10%}	1.0	73.6	/	0.5	877	17.6/300/0.059	98.0	[S8]
S/C _{FS}	1.0	80	40	0.3	1252	18.0/500/0.036	99.9	[S9]
20PVPS	1.5	78	15	1.0	859.8	46.5/500/0.093	/	[S10]
S@pPAN	1.0	55	/	1.0	795	10.6/200/0.053	~100	[S11]
c-PIL@S	1.0	59	38	0.5	1035.5	31.3/300/0.104	98.9	This work

Table S2. Fitted impedance values of Li||S and PIL@Li||*c*-PIL@S batteries after the 1st cycle and 100th cycle.

Battery	Li S		PIL@Li <i>c</i> -PIL@S	
Impedance	R _{SEI} (Ω)	R _{ct} (Ω)	R _{SEI} (Ω)	R _{ct} (Ω)
1 st	16.07	9.38	26.60	11.43
100 th	51.21	36.77	29.95	17.69

References

1. J. W. Feng, H. Yi, Z. W. Lei, J. Wang, H. B. Zeng, Y. H. Deng and C. Y. Wang, *J. Energy Chem.*, 2021, **56**, 171-178.
2. G. Yu, G. Ye, C. Wang, C. Wang, Z. Wang, P. Hu, Y. Li, X. X. Feng, S. J. Tan, M. Yan, S. Xin and Z. Liu, *Sci. China Chem.*, 2023, **66**, DOI:10.1007/s11426-023-1808-2.
3. G. W. Yu, C. Y. Wang, W. Dong, Y. W. Tian, Z. Wang, J. Lu, P. Hu, Y. Liu, M. Yan, Y. Li and Z. T. Liu, *J. Colloid Interface Sci.*, 2024, **654**, 201-211.
4. F. H. Wang, J. J. Wan, J. Liu, R. F. Wang and L. Wang, *Chem. Eng. Sci.*, 2023, **282**, 119294.
5. V. K. Tiwari, H. Song, Y. Oh and Y. Jeong, *Energy*, 2020, **195**, 117034.
6. B. Wei, Y. Tu, Y. Xia, W. Theis, J. Zhang, Z. Xu, S. Chen, J. Chen, G. Yin and H. L. Wang, *Chem. Eng. J.*, 2023, **473**, 144887.
7. X. Wang, B. Y. Guo, L. Liu, F. Zhang, C. Xia, L. Cui and F. Yang, *Electrochim. Acta*, 2023, **441**, 141857.
8. S. Wang, Y. Wu, M. Yang, L. Sun, Y. Tao and C. A. Yang, *New J. Chem.*, 2024, **48**, 621-630.
9. H. Li, X. Wu, S. Jiang, Q. Zhang, Y. Cao, H. Yang, F. Cao and X. Ai, *Nano Res.*, 2022, **16**, 8360-8367.
10. B. Long, J. Ma, T. Song, L. Liu, X. Wang, S. Song and Y. Tong, *Chem. Eng. J.*, 2021, **414**, 128799.
11. J. Lei, J. Chen, H. Zhang, A. Naveed, J. Yang, Y. Nuli and J. Wang, *ACS Appl. Mater. Interfaces*, 2020, **12**, 33702-33709.